

Probing the chemical complexity of amines in the ISM: detection of vinylamine (C₂H₃NH₂) and tentative detection of ethylamine (C₂H₅NH₂)

SHAOSHAN ZENG,¹ IZASKUN JIMÉNEZ-SERRA,² VÍCTOR M. RIVILLA,^{2,3} JESÚS MARTÍN-PINTADO,²
LUCAS F. RODRÍGUEZ-ALMEIDA,² BELÉN TERCERO,⁴ PABLO DE VICENTE,⁴ FERNANDO RICO-VILLAS,² LAURA COLZI,^{2,3}
SERGIO MARTÍN,^{5,6} AND MIGUEL A. REQUENA-TORRES^{7,8}

¹Star and Planet Formation Laboratory, Cluster for Pioneering Research, RIKEN, 2-1 Hirosawa, Wako, Saitama, 351-0198, Japan

²Centro de Astrobiología (CSIC-INTA), Ctra. Ajalvir km 4, Torrejón de Ardoz, 28850, Madrid, Spain

³INAF-Osservatorio Astrofisico di Arcetri, Largo E. Fermi 5, I-50125, Florence, Italy

⁴Observatorio de Yebes (IGN), Cerro de la Palera s/n, 19141, Guadalajara, Spain

⁵European Southern Observatory, Alonso de Córdova 3107, Vitacura 763 0355, Santiago, Chile

⁶Joint ALMA Observatory, Alonso de Córdova 3107, Vitacura 763 0355, Santiago, Chile

⁷University of Maryland, College Park, ND 20742-2421, USA

⁸Department of Physics, Astronomy and Geosciences, Towson University, MD 21252, USA

(Received -; Revised -; Accepted -)

Submitted to ApJL

ABSTRACT

Amines, in particular primary amines (R-NH₂) are closely related to the primordial synthesis of amino acids since they share the same structural backbone. However, only limited number of amines has been identified in the ISM which prevents us from studying their chemistry as well as their relation to pre-biotic species that could lead to the emergence of life. In this letter, we report the first interstellar detection of vinylamine (C₂H₃NH₂) and tentative detection of ethylamine (C₂H₅NH₂) towards the Galactic Centre cloud G+0.693-0.027. The derived abundance with respect to H₂ is $(3.3\pm 0.4)\times 10^{-10}$ and $(1.9\pm 0.5)\times 10^{-10}$, respectively. The inferred abundance ratios of C₂H₃NH₂ and C₂H₅NH₂ with respect to methylamine (CH₃NH₂) are ~ 0.02 and ~ 0.008 respectively. The derived abundance of C₂H₃NH₂, C₂H₅NH₂ and several other NH₂-bearing species are compared to those obtained towards high-mass and low-mass star-forming regions. Based on recent chemical and laboratory studies, possible chemical routes for the interstellar synthesis of C₂H₃NH₂ and C₂H₅NH₂ are discussed.

Keywords: Astrochemistry — Chemical abundance — Interstellar molecules — Galactic Centre

1. INTRODUCTION

The term prebiotic molecules refers to species that are considered to be involved in the processes leading to the origin of life. From the prospective of understanding the prebiotic chemistry in the interstellar medium (ISM), primary amines have caught much attention because they contain the same NH₂ group as those considered to be the fundamental building blocks of life (e.g. amino acids, nucleobases, nucleotides and other biochemical compounds). Although the attempts to observe glycine (NH₂CH₂COOH), the sim-

plest amino acid, in the ISM have not succeeded (e.g. Ceccarelli et al. 2000; Belloche et al. 2013), an increasing number of NH₂-bearing species have been reported in the last few years, which increases the chance to discover pre-biotic complex organics in space. This is in fact well-demonstrated towards G+0.693-0.027 (hereafter G+0.693), a molecular cloud located within the Sgr B2 complex in the Galactic Centre. As revealed by the census of N-bearing species towards G+0.693 (Zeng et al. 2018), several species containing NH₂ such as cyanamide (NH₂CN), formamide (NH₂CHO), and methylamine (CH₃NH₂) have been detected with abundance $\geq 10^{-9}$. Following the search, two key precursors in the synthesis of prebiotic nucleotides, hydroxylamine (NH₂OH) and urea (NH₂CONH₂) have also been identi-

fied towards G+0.693 (Rivilla et al. 2020; Jiménez-Serra et al. 2020). The very recent discovery of by far the most complex amine, ethanolamine ($\text{NH}_2\text{CH}_2\text{CH}_2\text{OH}$), the simplest head group of phospholipids in cell membranes, towards G+0.693 attests the potential of this source for finding more complex molecules of prebiotic relevance (Rivilla et al. 2021). This has thus prompted us to keep hunting for more amines in order to understand the chemical processes yielding related ingredients for life in space.

Structurally analogous to amino acids, CH_3NH_2 is the only primary amine that has been unambiguously observed towards different astronomical objects (e.g. Kaifu et al. 1974; Zeng et al. 2018; Bøgelund et al. 2019; Ohishi et al. 2019). Vinylamine (also known as ethenamine, $\text{C}_2\text{H}_3\text{NH}_2$) and ethylamine ($\text{C}_2\text{H}_5\text{NH}_2$) have not yet been reported in the ISM although the latter has been identified in multiple meteorites (Aponte et al. 2020, and references therein) and materials returned by the *Stardust* mission from comet 81P/Wild 2 (e.g. Glavin et al. 2008). Due to some concerns on the possible contamination of the stardust sample, their cometary origin could not be confirmed until the robust detection in the coma of comet 67P/Churyumov-Gerasimenko (Altwegg et al. 2016). The detection of CH_3NH_2 and $\text{C}_2\text{H}_5\text{NH}_2$ together with glycine in these solar system objects enhanced the probability of amino acids being formed in space. Indeed, the retrosynthesis of amino acids revealed that molecules containing the $-\text{NH}_2$ functional group are likely precursors of amino acids (Förstel et al. 2017). For example, CH_3NH_2 and $\text{C}_2\text{H}_5\text{NH}_2$ may be the major constituent of glycine and alanine ($\text{NH}_2\text{CH}_2\text{CHCOOH}$) respectively. According to the detailed quantum chemical calculation, $\text{C}_2\text{H}_3\text{NH}_2$ is the next energetically stable isomer in $\text{C}_2\text{H}_5\text{N}$ group after E- and Z- conformer of ethanimine (CH_3CHNH) (Sil et al. 2018), both of which have been detected in Sgr B2 (Loomis et al. 2013) as well as in G+0.693 (Rivilla et al. in prep.). $\text{C}_2\text{H}_5\text{NH}_2$ exists in two forms: anti- and gauche-conformer. The former is known to be more stable and has the higher expected intensity ratio than the latter conformer (see Sil et al. 2018, for details). Therefore anti- $\text{C}_2\text{H}_5\text{NH}_2$ should be the most viable candidate for the astronomical detection in the $\text{C}_2\text{H}_7\text{N}$ group. In this letter, we present the first detection of $\text{C}_2\text{H}_3\text{NH}_2$ and tentative detection of $\text{C}_2\text{H}_5\text{NH}_2$ in the ISM towards G+0.693 through the identification of several rotational transitions of its millimeter spectrum.

2. OBSERVATIONS

We have carried out high-sensitivity spectral surveys at 7, 3, and 2 mm towards G+0.693 molecular cloud us-

ing the IRAM 30m¹ and Yebes 40m² telescopes. The observations were centred at $\alpha(\text{J2000}) = 17^{\text{h}}47^{\text{m}}22^{\text{s}}$, $\delta(\text{J2000}) = -28^{\circ}21'27''$. The position switching mode was used in all observations with the reference position located at $\Delta\alpha, \Delta\delta = -885'', 290''$ with respect to the source position. The half-power beam width (HPBW) of the IRAM 30m and Yebes 40m telescope are in a range of $14''\text{--}36''$ at observed frequencies between 30 GHz and 175 GHz. The intensity of the spectra was measured in unit of antenna temperature, T_{A}^* as the molecular emission toward G+0.693 is extended over the beam (Zeng et al. 2020). The IRAM 30 m observations were performed in three observing runs during 2019: April 10-16, August 13-19 and December 11-15, from projects numbers 172-18 (PI Martín-Pintado), 018-19 (PI Rivilla) and 133-19 (PI Rivilla). It covered spectral ranges of 71.76-116.72 GHz and 124.77-175.5 GHz. We refer to Rivilla et al. (2020) for a full description of the IRAM 30 m observations. The Yebes 40 m observations were carried out during 6 observing sessions in February 2020, as part of the project 20A008 (PI Jiménez-Serra). The new Q band (7mm) HEMT receiver was used to allow broad-band observations in two linear polarisations. The spectral coverage ranges from 31.075 GHz to 50.424 GHz. We refer to Zeng et al. (2020) and Rivilla et al. (2020) for more detailed information on the Yebes 40 m observations.

3. ANALYSIS AND RESULTS

The line identification and analysis were carried out using the SLIM (Spectral Line Identification and Modelling) tool implemented within the MADCUBA package³(version 21/12/2020, Martín et al. 2019). The spectroscopic information of $\text{C}_2\text{H}_3\text{NH}_2$, within 0^+ & 0^- (CDMS⁴ entry 43504) was obtained from Brown et al. (1990) and Mcnaughton & Robertson (1994). And the spectroscopic information of $\text{C}_2\text{H}_5\text{NH}_2$, anti-conformer (CDMS entry 45515) was obtained from Fischer & Bot Skor (1982) and Apponi et al. (2008). Table 1 summarises the unblended or only partially blended transitions of $\text{C}_2\text{H}_3\text{NH}_2$ and $\text{C}_2\text{H}_5\text{NH}_2$ detected towards G+0.693. Note that all the $\text{C}_2\text{H}_5\text{NH}_2$ lines in Table 1 are a-type transitions with selection rules of $\Delta K_a=0$ and $\Delta K_c=\pm 1$. The rotational spectrum of $\text{C}_2\text{H}_3\text{NH}_2$

¹ IRAM is supported by INSU/CNRS (France), MPG (Germany), and IGN (Spain)

² http://rt40m.oan.es/rt40m_en.php

³ Madrid Data Cube Analysis on ImageJ is a software developed at the Center of Astrobiology (CAB) in Madrid; <http://cab.inta-csic.es/madcuba/Portada.html>.

⁴ Cologne Database for Molecular Spectroscopy (Endres et al. 2016). <https://cdms.astro.uni-koeln.de/classic/>

Table 1. List of observed transitions of C₂H₃NH₂ and C₂H₅NH₂. The following parameters are obtained from the CDMS catalogue entry 43504 and 45515: frequencies, quantum numbers, upper state degeneracy (g_u), the logarithm of the Einstein coefficients ($\log A_{ul}$), and the energy of the upper levels (E_u). The derived root mean square (rms) of the analysed spectra region, integrated intensity ($\int T_A^* dv$), signal-to-noise ratio (S/N), and the information about the species with transitions slightly blended with C₂H₃NH₂ or C₂H₅NH₂ lines are provided in the last column.

Frequency (GHz)	Transition (J _{K_a,K_c)}	$\log A_{ul}$ (s ⁻¹)	g_u	E_u (K)	rms (mK)	$\int T_A^* dv$ (mK km s ⁻¹)	S/N ^a	Blending
C ₂ H ₃ NH ₂								
92.31229	5 _{0,5} -4 _{0,4} ,0 ⁺	-5.31611	11	13.3	1.2	325	46	aGg-(CH ₂ OH) ₂
92.31539	5 _{0,5} -4 _{0,4} ,0 ⁻	-5.41309	11	78.3	1.2	8		
*92.92085	5 _{2,4} -4 _{2,3} ,0 ⁺	-5.38264	11	22.4	1.3	170	22	clean
*96.51369	5 _{1,4} -4 _{1,3} ,0 ⁺	-5.27533	11	16.1	2.5	282	19	clean
112.62479	6 _{2,4} -5 _{2,3} ,0 ⁺	-5.10095	13	27.8	5.7	198	6	g-C ₂ H ₅ SH
*128.32030	7 _{0,7} -6 _{0,6} ,0 ⁺	-4.87614	15	24.7	8.7	350	7	clean
*129.92445	7 _{2,6} -6 _{2,5} ,0 ⁺	-4.89588	15	33.9	6.8	200	5	clean
*146.03934	8 _{0,8} -7 _{0,7} ,0 ⁺	-4.70420	17	31.7	2.9	316	20	clean
149.14290	8 _{3,6} -7 _{3,5} ,0 ⁺	-4.74122	17	52.4	2.9	93	6	CH ₃ C ¹³ CH
159.88701	9 _{1,9} -8 _{1,8} ,0 ⁺	-4.58763	19	40.7	5.3	241	9	C ₂ H ₅ CN
C ₂ H ₅ NH ₂								
*32.14604	2 _{1,2} -1 _{1,1} ,0 ⁻	-6.88737	15	3.4	1.1	8		
*32.14605	2 _{1,2} -1 _{1,1} ,0 ⁺	-6.88739	45	3.4	1.1	24	4	clean
*34.04659	2 _{1,1} -1 _{1,0} ,0 ⁻	-6.81259	15	3.5	1.2	8		
*34.04662	2 _{1,1} -1 _{1,0} ,0 ⁺	-6.81261	45	3.5	1.2	25	4	clean
*49.52875	3 _{0,3} -2 _{0,2} ,0 ⁺	-6.16968	63	4.7	2.8	67		
*49.52875	3 _{0,3} -2 _{0,2} ,0 ⁻	-6.16966	21	4.7	2.8	22	6	clean
82.16878	5 _{0,5} -4 _{0,4} ,0 ⁺	-5.48528	99	11.8	2.8	109		
82.16878	5 _{0,5} -4 _{0,4} ,0 ⁻	-5.48526	33	11.8	2.8	36	8	¹³ CH ₃ CH ₂ OH
*83.24287	5 _{2,3} -4 _{2,2} ,0 ⁺	-5.54312	99	16.4	3.1	64		
*83.24287	5 _{2,3} -4 _{2,2} ,0 ⁻	-5.54310	33	16.4	3.1	21	4	clean
84.98078	5 _{1,4} -4 _{1,3} ,0 ⁺	-5.45828	99	13.3	3.3	96		
84.98078	5 _{1,4} -4 _{1,3} ,0 ⁻	-5.45826	33	13.3	3.3	32	6	H ¹⁵ NCO
145.87174	9 _{0,9} -8 _{0,8} ,0 ⁺	-4.72105	171	35.3	2.3	56		
145.87174	9 _{0,9} -8 _{0,8} ,0 ⁻	-4.72103	57	35.3	2.3	19	6	S ¹⁸ O

^a S/N is calculated as: $(\int T_A^* dv) / [\text{rms}(\frac{\Delta\nu}{\text{FWHM}})^{0.5} \text{FWHM}]$, where $\Delta\nu$ is the spectral resolution of the data, range between 1.5 and 2.2 km s⁻¹. The clean transitions are denoted by an asterisk. A single common S/N is given for the overlapping transitions.

and C₂H₅NH₂ are characterised by inversion doubling due to the large amplitude inversion motion of the NH₂ group. Each rotational energy level, specified by the rotational quantum numbers J and K, is thus split into an inversion doublet. The 0⁺ or 0⁻ in Table 1 indicate the inversion doublet from which the transition arises. For C₂H₅NH₂, the variation of upper state degeneracy and integrated intensity of the same transition is due to the spin statistical weight of 3:1 between the symmetric and anti-symmetric sub-levels.

The analysis was performed under the assumption of local thermodynamic equilibrium (LTE) conditions due to the lack of collisional coefficients of C₂H₃NH₂ and C₂H₅NH₂. Due to the low density of G+0.693 ($\sim 10^4$ - 10^5 cm⁻³; Zeng et al. 2020), molecules are sub-thermally excited in the source and hence their excitation temper-

atures (in a range of 5 to 20 K; e.g. Requena-Torres et al. 2008; Rivilla et al. 2018; Zeng et al. 2018) are significantly lower than the kinetic temperature of the source (~ 150 K; e.g. Zeng et al. 2018). However, note that the transitions of C₂H₃NH₂ and C₂H₅NH₂ are well fitted using one excitation temperature for each species. Considering the effect of line opacity, MADCUBA-SLIM generated synthetic spectra that can be compared to the observed spectra. The MADCUBA-AUTOFIT tool was then used to provide the best non-linear least-squares LTE fit to the data using the Levenberg-Marquardt algorithm. It is important to note that not a single transition of C₂H₃NH₂ and C₂H₅NH₂ predicted by the LTE spectrum is missing in the data. To properly evaluate the line contamination by other molecules, over 300 species have been searched for in our dataset. This included

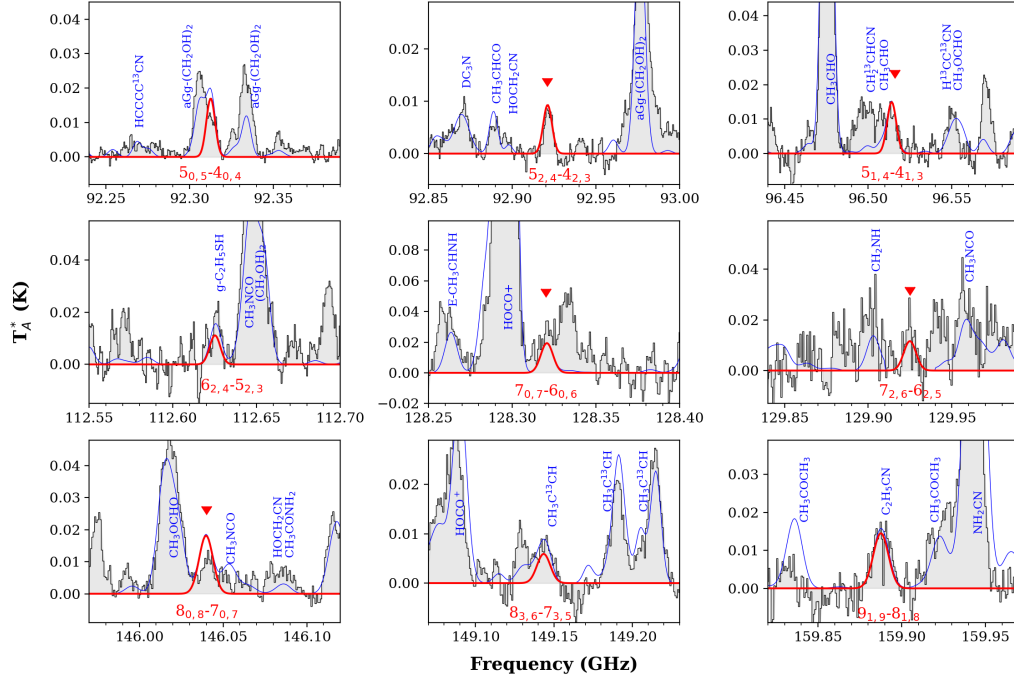


Figure 1. Unblended or only slightly blended transitions of $C_2H_3NH_2$ detected towards G+0.693. The red line shows the best LTE fit to the $C_2H_3NH_2$ lines while the blue line shows the total contribution, including the emission from other molecular species (labelled) identified in G+0.693. The cleanest detected transitions are denoted by a red \blacktriangledown .

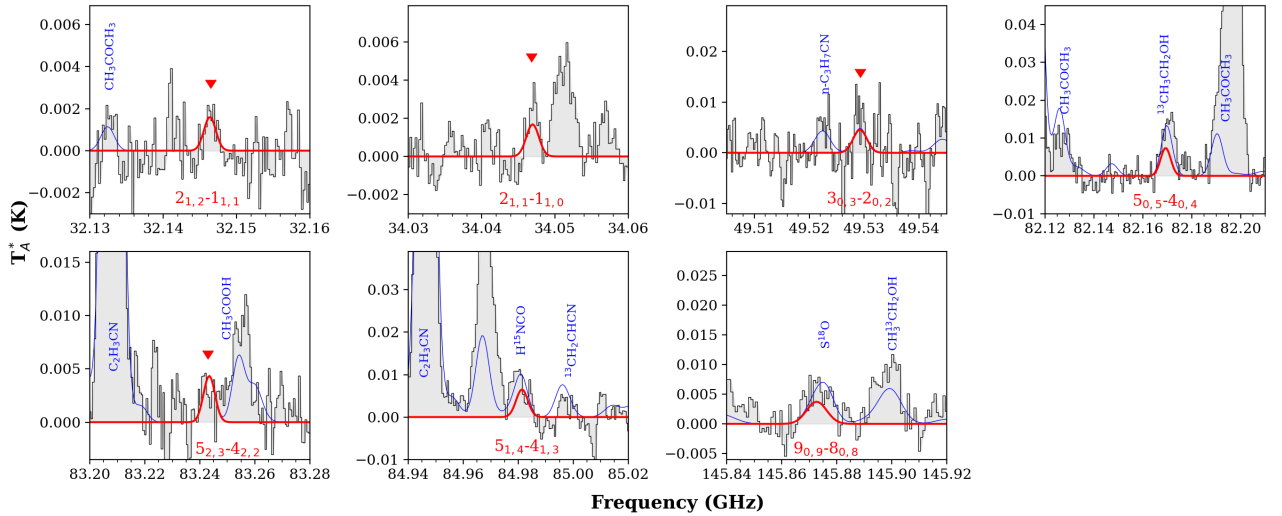


Figure 2. Unblended or only slightly blended transitions tentatively identified for $C_2H_5NH_2$ towards G+0.693. The cleanest transitions are denoted by a red \blacktriangledown .

not only all the molecules detected towards G+0.693 in previous studies (Requena-Torres et al. 2008; Zeng et al. 2018; Rivilla et al. 2018, 2019, 2020, 2021; Jiménez-Serra et al. 2020; Rodríguez-Almeida et al. 2021), but also those reported in the ISM⁵. The molecule blended

with the transition of $C_2H_3NH_2$ and $C_2H_5NH_2$ is listed in the last column of Table 1. We note that the line identification and fitting file used in this analysis is the same as the one used in previous works (e.g. Zeng et al. 2018; Rodríguez-Almeida et al. 2021) as well as on-going works. Therefore, the excitation temperatures and column densities of blending species are consistent with the ones reported in all these studies.

⁵ See <https://cdms.astro.uni-koeln.de/classic/molecules>

For C₂H₃NH₂, we detect five clean transitions and four slightly blended transitions with a blending contribution of <10% (see Figure 1). For C₂H₅NH₂, only four clean transitions are reported and three are slightly blended (Figure 2). Since the clean transitions of C₂H₅NH₂ are weak (S/N=4 in integrated intensity; Table 1), we conclude that this species is tentatively detected. The free parameters that can be fitted are: molecular column density (N_{tot}), excitation temperature (T_{ex}), radial velocity (V_{LSR}), full width half maximum ($FWHM$, $\Delta\nu$), and source size (θ). For G+0.693, we assumed that the source size is extended in MAD-CUBA. As the algorithm did not converge when fitting C₂H₃NH₂ with all parameters left free, we fixed the $FWHM$ and V_{LSR} to 18 km s⁻¹ and 67 km s⁻¹ respectively by visual inspection of the most unblended lines. These values are consistent with those from many other molecules previously analysed in G+0.693 ($FWHM \sim 20$ km s⁻¹, $V_{\text{LSR}} \sim 68$ km s⁻¹; Requena-Torres et al. 2008; Zeng et al. 2018; Rivilla et al. 2018, 2019, 2020; Jiménez-Serra et al. 2020; Rodríguez-Almeida et al. 2021). The resulting LTE fit gives $T_{\text{ex}}=(18\pm 3)$ K and $N_{\text{tot}}=(4.5\pm 0.6)\times 10^{13}$ cm⁻². In the case of C₂H₅NH₂, the V_{LSR} was fixed to 67 km s⁻¹ and the LTE fit gives $T_{\text{ex}}=(12\pm 5)$ K, $FWHM=(18\pm 5)$ km s⁻¹ and $N_{\text{tot}}=(2.5\pm 0.7)\times 10^{13}$ cm⁻².

The resulting best LTE fit to the C₂H₃NH₂ and C₂H₅NH₂ lines is shown in red line in Fig.1 and Fig.2 whilst blue line indicates the best fit considering also the total contribution of the LTE emission from all the other identified molecules. Adapting the H₂ column density inferred from observations of C¹⁸O ($N_{\text{H}_2} = 1.35\times 10^{23}$ cm⁻²; Martín et al. 2008), the resulting abundance is $(3.3\pm 0.4)\times 10^{-10}$ and $(1.9\pm 0.5)\times 10^{-10}$ for C₂H₃NH₂ and C₂H₅NH₂ respectively.

4. DISCUSSION

Figure 3 presents the abundance with respect to H₂, in decreasing order, of NH₂-bearing species detected towards G+0.693. The results are compared to those derived towards three high-mass and low-mass star-forming regions that are chemically rich, i.e. Sgr B2(N), Orion KL, and IRAS 16293-2422 B. The low abundance or non-detection of -NH₂ species may indicate that their formation is less efficient towards Orion KL and IRAS 16293-2422 B. On the other hand, the detection with abundance $>10^{-11}$ suggests G+0.693 is a prominent -NH₂ molecule repository which allows us to study their origin as well as their chemical relation to other prebiotic molecules.

In contrast to the three compared sources, G+0.693 lacks an internal heating source responsible for the rich

chemistry. The high level of molecular complexity is attributed to dust grain sputtering by low-velocity shocks (≤ 20 km s⁻¹), which is driven by the possible cloud-cloud collision occurring in the Sgr B2 complex (Zeng et al. 2020). This is indicated by the high abundances of shock tracers such as HNCO and SiO (Martín et al. 2008; Rivilla et al. 2018) and the presence of molecules that are known to be formed on grain surfaces (Requena-Torres et al. 2008; Zeng et al. 2018). In addition, the abundance ratio of HC₃N/HC₅N and C₂H₃CN/C₂H₅CN derived in Zeng et al. (2018) suggested that an enhanced cosmic-ray ionisation rate may also play a role in the chemistry of N-bearing species towards G+0.693. In the following Section, we evaluate the possible formation routes for the amines detected towards G+0.693 and the discussed formation routes are summarised in Figure 4.

4.1. Formation of primary amines

Despite the low number of detections in the ISM, the CH₃NH₂ chemistry under astrophysical conditions has been studied in theoretical, experimental and chemical modelling work. In the gas-phase, CH₃NH₂ is proposed to form via the radiative association between ammonia (NH₃) and the methyl radical cation (CH₃⁺) followed by recombination dissociation (Herbst 1985). On the grain surfaces, experimental work demonstrated that CH₃NH₂ can form via sequential hydrogenation of hydrogen cyanide (HCN): HCN → CH₂NH → CH₃NH₂ (Theule et al. 2011). Alternatively, gas-grain chemical model by Garrod et al. (2008) has suggested that CH₃NH₂ is formed by simple addition of CH₃ from CH₄ to azanyl radical (NH₂) from NH₃ during warm-up phases. This radical-radical recombination has recently been studied in laboratory ice simulations revealing that CH₃NH₂ can be synthesised in irradiated ices composed of CH₄ and NH₃ (Kim & Kaiser 2011; Förstel et al. 2017) but also in cold and quiescent molecular clouds (Ioppolo et al. 2021). On the contrary, little is known about the chemistry of C₂H₃NH₂ and C₂H₅NH₂.

C₂H₅NH₂: Although there are no chemical routes included in current astrochemical databases, different formation mechanisms of C₂H₅NH₂ have been discussed in the literature. For instance, the addition of the CH₃ radical to CH₂NH followed by hydrogenation of the resulting product would produce C₂H₅NH₂ on grain surfaces (Bernstein et al. 1995); the photochemistry of a mixture of ethylene (C₂H₄) and NH₃ in which C₂H₅NH₂ is formed from radical-radical reaction of the ethyl radical (C₂H₅) with NH₂ (Danger et al. 2011, and references therein). Reactions of CH₃NH₂ with carbene (CH₂) or ethane (C₂H₆) with nitrene (NH) are also expected to form C₂H₅NH₂, but with lower probability

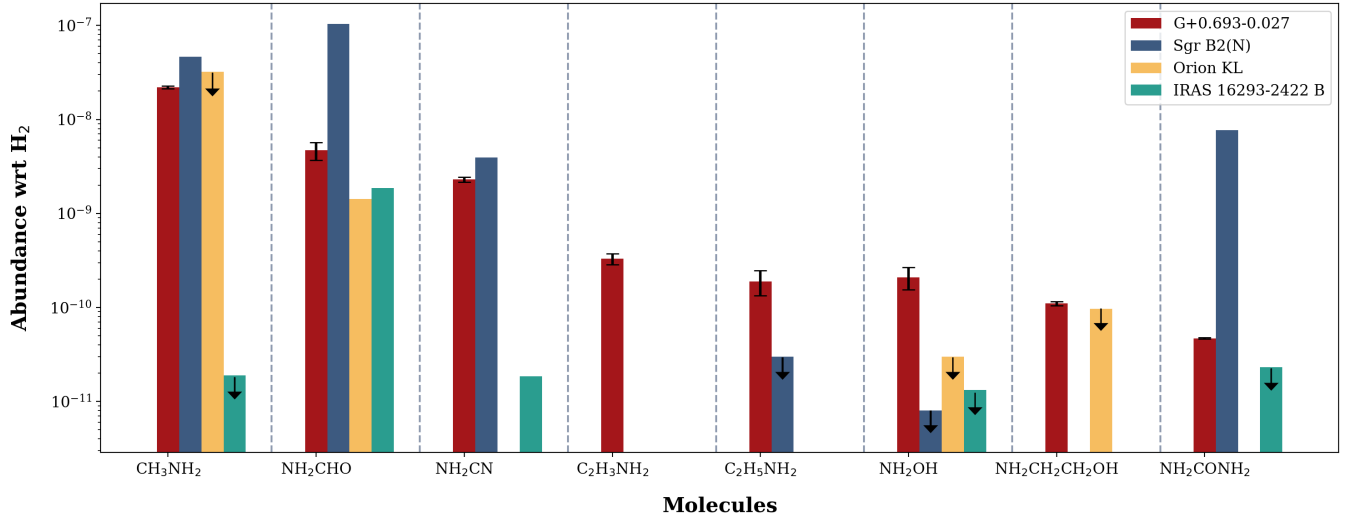


Figure 3. Derived abundance of NH₂-bearing species with respect to H₂ towards G+0.693-0.027, Sgr B2(N), Orion KL, and IRAS 16293-2422 B. For G+0.693-0.027 ($N(\text{H}_2)=1.35 \times 10^{23} \text{ cm}^{-2}$; Martín et al. 2008), molecular column densities are obtained from this work, Zeng et al. (2018); Jiménez-Serra et al. (2020); Rivilla et al. (2020) and Rivilla et al. (2021). For IRAS 16293-2422 B ($N(\text{H}_2)=2.8 \times 10^{25} \text{ cm}^{-2}$; Martín-Doménech et al. 2017), molecular column densities are from Martín-Doménech et al. (2017); Ligterink et al. (2018) and Jiménez-Serra et al. (2020). For Sgr B2(N): CH₃NH₂, NH₂CHO, and NH₂CN from Belloche et al. (2013) with $N(\text{H}_2)=1.3 \times 10^{25} \text{ cm}^{-2}$ (Belloche et al. 2008); abundance of C₂H₅NH₂ and upper limit of NH₂OH is taken directly from Apponi et al. (2008) and Pulliam et al. (2012) respectively; NH₂CONH₂ is derived from Belloche et al. (2019) by assuming Sgr B2(N1S) has the same $N(\text{H}_2)=3.5 \times 10^{24} \text{ cm}^{-2}$ (Li et al. 2021) as Sgr B2 (N1E). For Orion KL: column density of CH₃NH₂ and $N(\text{H}_2)=3.1 \times 10^{23} \text{ cm}^{-2}$ are from Pagani et al. (2017); NH₂CHO from Motiyenko et al. (2012) with $N(\text{H}_2)=4.2 \times 10^{23} \text{ cm}^{-2}$ Tercero et al. (2010); upper limits of NH₂OH and NH₂CH₂CH₂OH are from Pulliam et al. (2012) and Wiström et al. (2007) respectively with $N(\text{H}_2)=7.0 \times 10^{23} \text{ cm}^{-2}$ (Womack et al. 1992).

(Förstel et al. 2017). More recently, experimental simulation of interstellar ice analogs containing CH₃NH₂ revealed that C₂H₅NH₂ can be formed efficiently from CH₃ and methanamine radical (CH₂NH₂) (Carrascosa et al. 2021).

In addition to the aforementioned formation pathways, one might also expect C₂H₅NH₂ to be formed through the same mechanism as suggested for CH₃NH₂: successive hydrogenation starting from acetonitrile (CH₃CN): CH₃CN → CH₃CHNH → C₂H₅NH₂. However, CH₃CN has been proposed to be a product of the surface chemistry of CH₃NH₂ (Carrascosa et al. 2021). Furthermore, laboratory work showed that CH₃CN does not react with H atoms between 10 and 60 K (Nguyen et al. 2019). Considering the temperature of dust grains in G+0.693 is $T_{\text{dust}} \leq 30 \text{ K}$ (Zeng et al. 2018, and reference therein), this proposed hydrogenation leading to C₂H₅NH₂ is unlikely to occur on dust grains in G+0.693. Based on the reaction rate coefficients provided in Sil et al. (2018), C₂H₅NH₂ is less likely produced in the same hydrogenation reaction in the gas phase due to its low efficiency at typical kinetic temperature in Galactic Centre clouds, $T_{\text{kin}} = 50\text{--}120 \text{ K}$ (Zeng et al. 2018, and reference therein). To our best knowledge, with no other possible gas phase reaction to form C₂H₅NH₂, this species likely forms on the surface of dust grains in

G+0.693. Regardless the chemical formation route on grains, the sputtering of grain icy mantles by large-scale low-velocity ($\leq 20 \text{ km s}^{-1}$) shocks in G+0.693 would release C₂H₅NH₂ into gas phase from grains (see e.g. Requena-Torres et al. 2008; Martín et al. 2008; Zeng et al. 2020).

C₂H₃NH₂: With the available reaction rate coefficients in the Kinetic Database for Astrochemistry (KIDA, Wakelam et al. 2012), C₂H₃NH₂ is proposed to form from the reaction between the CH radical and CH₃NH₂ in the gas-phase, most efficient at temperatures $T=50\text{--}200 \text{ K}$. With $T_{\text{kin}} = 50\text{--}120 \text{ K}$, C₂H₃NH₂ is thus expected to be formed efficiently via this pathway in G+0.693. In particular, CH₃NH₂ is found to be abundant ($\sim 10^{-8}$; Zeng et al. 2018) in G+0.693 which would be readily available for this chemical reaction to proceed. Another possible gas-phase formation route is through the reaction involving C₂H₅NH₂ + H⁺ or H₃⁺ followed by recombination dissociation, analogous to the formation of C₂H₃CN from C₂H₅CN proposed by Caselli et al. (1993). As discussed in Zeng et al. (2018) for -CN group species, this ion-molecule gas-phase reaction can be efficient thanks to (i) the presence of high cosmic ray ionisation rate in the Galactic Centre and (ii) the relatively low densities of $\sim 10^4 \text{ cm}^{-3}$ of G+0.693. This, and the fact that a similar abundance

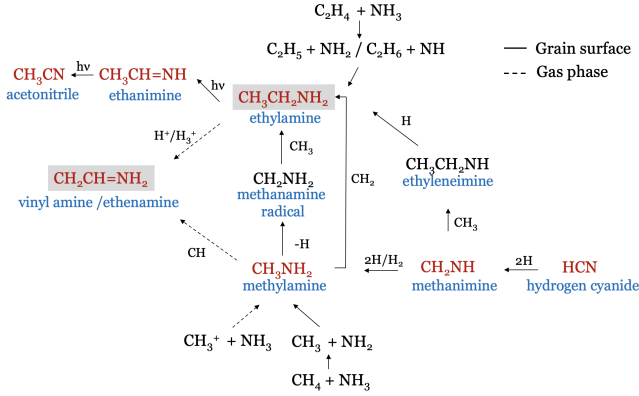


Figure 4. Summary of the chemical routes proposed for the formation of C₂H₃NH₂ and C₂H₅NH₂ in the ISM. The molecular species in red are those that have been detected towards G+0.693. The solid arrows denote surface chemistry reactions and dashed arrows denote gas-phase chemistry.

ratios are found for C₂H₃CN/C₂H₅CN = 2.2±0.3 and C₂H₃NH₂/C₂H₅NH₂=1.7±0.5 towards G+0.693, makes this formation route plausible.

On the grain surface, C₂H₃NH₂ might be a photoproduct of C₂H₅NH₂ (Hamada et al. 1984). But recent experimental investigation showed that its isomer, ethanimine (CH₃CHNH), appears to be the primary product of photolysis of C₂H₅NH₂ (Danger et al. 2011). This has also been recently found by Carrascosa et al. (2021), who even synthesised large N-heterocycles in interstellar ice analogs under UV radiation. We thus propose that the formation of C₂H₃NH₂ likely occurs in the gas phase towards G+0.693 although further theoretical or laboratory work is needed to determine the rate constant of the reaction C₂H₅NH₂ + H⁺/H₃⁺.

In summary, we report the discovery of two new amines in the ISM: C₂H₃NH₂ and tentatively C₂H₅NH₂. The abundance ratios with respect to CH₃NH₂ are ~0.02 and ~0.008, i.e. about a factor >10. This

trend has been found for other species such as ethanol (with respect to methanol) or ethyl cyanide (with respect to CH₃CN; Zeng et al. 2018; Rodríguez-Almeida et al. 2021). Primary amines are known to be involved in the synthesis of proteinogenic alpha-amino acids Förstel et al. (2017). Therefore, their discovery provides crucial information about the connection between interstellar chemistry and the prebiotic material found in meteorites and comets.

ACKNOWLEDGMENTS

The authors wish to thank the referees for constructive comments that significantly improved the paper. We are grateful to the IRAM 30-m and Yebes 40-m telescope staff for help during the different observing runs. IRAM is supported by the National Institute for Universe Sciences and Astronomy/National Center for Scientific Research (France), Max Planck Society for the Advancement of Science (Germany), and the National Geographic Institute (IGN) (Spain). The 40-m radio telescope at Yebes Observatory is operated by the IGN, Ministerio de Transportes, Movilidad y Agenda Urbana. This study is supported by a Grant-in-Aid from the Ministry of Education, Culture, Sports, Science, and Technology of Japan (20H05845) and by a RIKEN pioneering Project (Evolution of Matter in the Universe). We also acknowledge partial support from the Spanish National Research Council (CSIC) through the i-Link project number LINKA20353. I.J.-S. and J.M.-P. have received partial support from the Spanish State Research Agency through project number PID2019-105552RB-C41. V.M.R., L.R.-A., and L.C. have received funding from the Comunidad de Madrid through the Atracción de Talento Investigador (Doctores con experiencia) Grant (COOL: Cosmic Origins Of Life; 2019-T1/TIC-15379).

REFERENCES

- Altwegg, K., Balsiger, H., Bar-Nun, A., et al. 2016, *Science Advances*, 2, e1600285, doi: [10.1126/sciadv.1600285](https://doi.org/10.1126/sciadv.1600285)
- Aponte, J. C., Elsila, J. E., Hein, J. E., et al. 2020, *Meteoritics and Planetary Science*, 55, 2422, doi: [10.1111/maps.13586](https://doi.org/10.1111/maps.13586)
- Apponi, A. J., Sun, M., Halfen, D. T., Ziurys, L. M., & Müller, H. S. P. 2008, *ApJ*, 673, 1240, doi: [10.1086/523796](https://doi.org/10.1086/523796)
- Belloche, A., Garrod, R. T., Müller, H. S. P., et al. 2019, *A&A*, 628, A10, doi: [10.1051/0004-6361/201935428](https://doi.org/10.1051/0004-6361/201935428)
- Belloche, A., Menten, K. M., Comito, C., et al. 2008, *A&A*, 482, 179, doi: [10.1051/0004-6361:20079203](https://doi.org/10.1051/0004-6361:20079203)
- Belloche, A., Müller, H. S. P., Menten, K. M., Schilke, P., & Comito, C. 2013, *A&A*, 559, A47, doi: [10.1051/0004-6361/201321096](https://doi.org/10.1051/0004-6361/201321096)
- Bernstein, M. P., Sandford, S. A., Allamandola, L. J., Chang, S., & Scharberg, M. A. 1995, *ApJ*, 454, 327, doi: [10.1086/176485](https://doi.org/10.1086/176485)
- Bøgelund, E. G., McGuire, B. A., Hogerheijde, M. R., van Dishoeck, E. F., & Ligterink, N. F. W. 2019, *A&A*, 624, A82, doi: [10.1051/0004-6361/201833676](https://doi.org/10.1051/0004-6361/201833676)

- Brown, R. D., Godfrey, P. D., Kleibomer, B., Pierlot, A. P., & McNaughton, D. 1990, *Journal of Molecular Spectroscopy*, 142, 195, doi: [10.1016/0022-2852\(90\)90177-R](https://doi.org/10.1016/0022-2852(90)90177-R)
- Carrascosa, H., González Díaz, C., Muñoz Caro, G. M., Gómez, P. C., & Sanz, M. L. 2021, arXiv e-prints, arXiv:2106.05622. <https://arxiv.org/abs/2106.05622>
- Caselli, P., Hasegawa, T. I., & Herbst, E. 1993, *ApJ*, 408, 548, doi: [10.1086/172612](https://doi.org/10.1086/172612)
- Ceccarelli, C., Loinard, L., Castets, A., Faure, A., & Lefloch, B. 2000, *A&A*, 362, 1122
- Danger, G., Bossa, J. B., de Marcellus, P., et al. 2011, *A&A*, 525, A30, doi: [10.1051/0004-6361/201015736](https://doi.org/10.1051/0004-6361/201015736)
- Endres, C. P., Schlemmer, S., Schilke, P., Stutzki, J., & Müller, H. S. P. 2016, *Journal of Molecular Spectroscopy*, 327, 95, doi: [10.1016/j.jms.2016.03.005](https://doi.org/10.1016/j.jms.2016.03.005)
- Fischer, E., & Botskor, I. 1982, *Journal of Molecular Spectroscopy*, 91, 116, doi: [10.1016/0022-2852\(82\)90035-2](https://doi.org/10.1016/0022-2852(82)90035-2)
- Förstel, M., Bergantini, A., Maksyutenko, P., Góbi, S., & Kaiser, R. I. 2017, *ApJ*, 845, 83, doi: [10.3847/1538-4357/aa7edd](https://doi.org/10.3847/1538-4357/aa7edd)
- Garrod, R. T., Widicus Weaver, S. L., & Herbst, E. 2008, *ApJ*, 682, 283, doi: [10.1086/588035](https://doi.org/10.1086/588035)
- Glavin, D. P., Dworkin, J. P., & Sandford, S. A. 2008, *Meteoritics and Planetary Science*, 43, 399, doi: [10.1111/j.1945-5100.2008.tb00629.x](https://doi.org/10.1111/j.1945-5100.2008.tb00629.x)
- Hamada, Y., Hashiguchi, K., Tsuboi, M., Koga, Y., & Kondo, S. 1984, *Journal of Molecular Spectroscopy*, 105, 93, doi: [10.1016/0022-2852\(84\)90106-1](https://doi.org/10.1016/0022-2852(84)90106-1)
- Herbst, E. 1985, *ApJ*, 292, 484, doi: [10.1086/163179](https://doi.org/10.1086/163179)
- Ioppolo, S., Fedoseev, G., Chuang, K. J., et al. 2021, *Nature Astronomy*, 5, 197, doi: [10.1038/s41550-020-01249-0](https://doi.org/10.1038/s41550-020-01249-0)
- Jiménez-Serra, I., Martín-Pintado, J., Rivilla, V. M., et al. 2020, *Astrobiology*, 20, 1048, doi: [10.1089/ast.2019.2125](https://doi.org/10.1089/ast.2019.2125)
- Kaifu, N., Morimoto, M., Nagane, K., et al. 1974, *ApJL*, 191, L135, doi: [10.1086/181569](https://doi.org/10.1086/181569)
- Kim, Y. S., & Kaiser, R. I. 2011, *ApJ*, 729, 68, doi: [10.1088/0004-637X/729/1/68](https://doi.org/10.1088/0004-637X/729/1/68)
- Li, J., Wang, J., Lu, X., et al. 2021, arXiv e-prints, arXiv:2108.05001. <https://arxiv.org/abs/2108.05001>
- Ligterink, N. F. W., Calcutt, H., Coutens, A., et al. 2018, *A&A*, 619, A28, doi: [10.1051/0004-6361/201731980](https://doi.org/10.1051/0004-6361/201731980)
- Loomis, R. A., Zaleski, D. P., Steber, A. L., et al. 2013, *ApJL*, 765, L9, doi: [10.1088/2041-8205/765/1/L9](https://doi.org/10.1088/2041-8205/765/1/L9)
- Martín, S., Martín-Pintado, J., Blanco-Sánchez, C., et al. 2019, *A&A*, 631, A159, doi: [10.1051/0004-6361/201936144](https://doi.org/10.1051/0004-6361/201936144)
- Martín, S., Requena-Torres, M. A., Martín-Pintado, J., & Mauersberger, R. 2008, *ApJ*, 678, 245, doi: [10.1086/533409](https://doi.org/10.1086/533409)
- Martín-Doménech, R., Rivilla, V. M., Jiménez-Serra, I., et al. 2017, *MNRAS*, 469, 2230, doi: [10.1093/mnras/stx915](https://doi.org/10.1093/mnras/stx915)
- Mcnaughton, D., & Robertson, E. G. 1994, *Journal of Molecular Spectroscopy*, 163, 80, doi: [10.1006/jmsp.1994.1009](https://doi.org/10.1006/jmsp.1994.1009)
- Motiyenko, R. A., Tercero, B., Cernicharo, J., & Margulès, L. 2012, *A&A*, 548, A71, doi: [10.1051/0004-6361/201220033](https://doi.org/10.1051/0004-6361/201220033)
- Nguyen, T., Fouché, I., Favre, C., et al. 2019, *A&A*, 628, A15, doi: [10.1051/0004-6361/201935127](https://doi.org/10.1051/0004-6361/201935127)
- Ohishi, M., Suzuki, T., Hirota, T., Saito, M., & Kaifu, N. 2019, *PASJ*, 71, 86, doi: [10.1093/pasj/psz068](https://doi.org/10.1093/pasj/psz068)
- Pagani, L., Favre, C., Goldsmith, P. F., et al. 2017, *A&A*, 604, A32, doi: [10.1051/0004-6361/201730466](https://doi.org/10.1051/0004-6361/201730466)
- Pulliam, R. L., McGuire, B. A., & Remijan, A. J. 2012, *ApJ*, 751, 1, doi: [10.1088/0004-637X/751/1/1](https://doi.org/10.1088/0004-637X/751/1/1)
- Requena-Torres, M. A., Martín-Pintado, J., Martín, S., & Morris, M. R. 2008, *ApJ*, 672, 352, doi: [10.1086/523627](https://doi.org/10.1086/523627)
- Rivilla, V. M., Jiménez-Serra, I., Zeng, S., et al. 2018, *MNRAS*, 475, L30, doi: [10.1093/mnras/lsx208](https://doi.org/10.1093/mnras/lsx208)
- Rivilla, V. M., Martín-Pintado, J., Jiménez-Serra, I., et al. 2019, *MNRAS*, 483, L114, doi: [10.1093/mnras/sly228](https://doi.org/10.1093/mnras/sly228)
- . 2020, *ApJL*, 899, L28, doi: [10.3847/2041-8213/abac55](https://doi.org/10.3847/2041-8213/abac55)
- Rivilla, V. M., Jiménez-Serra, I., Martín-Pintado, J., et al. 2021, *Proceedings of the National Academy of Science*, 118, 2101314118, doi: [10.1073/pnas.2101314118](https://doi.org/10.1073/pnas.2101314118)
- Rodríguez-Almeida, L. F., Jiménez-Serra, I., Rivilla, V. M., et al. 2021, *ApJL*, 912, L11, doi: [10.3847/2041-8213/abf7cb](https://doi.org/10.3847/2041-8213/abf7cb)
- Sil, M., Gorai, P., Das, A., et al. 2018, *ApJ*, 853, 139, doi: [10.3847/1538-4357/aa984d](https://doi.org/10.3847/1538-4357/aa984d)
- Tercero, B., Cernicharo, J., Pardo, J. R., & Goicoechea, J. R. 2010, *A&A*, 517, A96, doi: [10.1051/0004-6361/200913501](https://doi.org/10.1051/0004-6361/200913501)
- Theule, P., Borget, F., Mispelaer, F., et al. 2011, *A&A*, 534, A64, doi: [10.1051/0004-6361/201117494](https://doi.org/10.1051/0004-6361/201117494)
- Wakelam, V., Herbst, E., Loison, J. C., et al. 2012, *ApJS*, 199, 21, doi: [10.1088/0067-0049/199/1/21](https://doi.org/10.1088/0067-0049/199/1/21)
- Wirström, E. S., Bergman, P., Hjalmarsen, Å., & Nummelin, A. 2007, *A&A*, 473, 177, doi: [10.1051/0004-6361:20077535](https://doi.org/10.1051/0004-6361:20077535)
- Womack, M., Ziurys, L. M., & Wyckoff, S. 1992, *ApJ*, 393, 188, doi: [10.1086/171496](https://doi.org/10.1086/171496)
- Zeng, S., Jiménez-Serra, I., Rivilla, V. M., et al. 2018, *MNRAS*, 478, 2962, doi: [10.1093/mnras/sty1174](https://doi.org/10.1093/mnras/sty1174)
- Zeng, S., Zhang, Q., Jiménez-Serra, I., et al. 2020, *MNRAS*, 497, 4896, doi: [10.1093/mnras/staa2187](https://doi.org/10.1093/mnras/staa2187)